

# Informational Corrections to the Early-Universe Radiation Sector: CET $\Omega$ , WIMP Freeze-Out, and Implications for a Possible 20 GeV Gamma-Ray Excess

Christian Balfagón<sup>1</sup>

*Universidad de Buenos Aires, Argentina*

---

## Abstract

Recent analyses of Fermi–LAT data have identified a nearly spherical, halo-like excess of gamma rays peaking at  $E_\gamma \sim 20$  GeV. If interpreted as dark matter annihilation, the excess directly probes the thermal freeze-out epoch, and therefore any non-standard corrections to the early-Universe expansion rate.

In this work we examine the implications of this tentative signal for CET  $\Omega$ , an informational and modular extension of relativistic quantum field theory and cosmology. CET  $\Omega$  predicts a universal, state-dependent modification to the radiation energy density,

$$\rho_\Omega(a) = \rho_r(a) [1 + \alpha_{\log} \log \log(a/a_i)],$$

originating from renormalized modular fluctuations in the spectral triple of the theory. The correction is negligible during BBN and CMB epochs, but becomes relevant during thermal WIMP freeze-out.

We provide: (i) a derivation of the doubly logarithmic correction from the modular two-point function; (ii) the physical justification of the onset scale  $a_i$  and its relation to the informational sector; (iii) the full quantitative impact on freeze-out, including numerical solutions; (iv) the evolution of the informational field  $\Phi_\Omega(x)$ , demonstrating that it freezes in at  $a_{\text{dec}} < a_f$  and survives to  $z = 0$  under gravitational advection; (v) the resulting sub-percent morphological modifications to the annihilation flux; (vi) a comparison with Early Dark Energy, kination, and varying- $N_{\text{eff}}$  models.

We show that the range  $10^{-4} \lesssim \alpha_{\log} \lesssim 10^{-2}$  is naturally selected by the theory, remains consistent with Planck, BBN, and BAO constraints, and induces percent-level shifts in the relic abundance while predicting potentially constrainable deviations in the gamma-ray morphology accessible to next-generation MeV–GeV missions.

*Keywords:* dark matter, cosmology, early Universe, gamma rays, WIMPs, modular theory, informational physics

---

## 1. Introduction

A series of independent analyses of Fermi–LAT data have reported a statistically significant, approximately spherical excess of gamma rays peaking at  $E_\gamma \sim 20$  GeV [1–6]. Although astrophysical scenarios remain viable, the morphology and spectral shape of the excess are consistent with annihilating WIMPs in the  $\sim 20$ –40 GeV mass range [7, 8].

If confirmed as a dark matter signal, such an excess would provide a direct observational window into the physics of thermal freeze-out and the expansion history of the early Universe. This makes indirect detection an especially sensitive probe of any non-standard cosmological evolution at temperatures above the MeV scale [7–9].

CET  $\Omega$  [10–12] provides a natural framework in which to explore such deviations, complementing the broad class of non-standard early-Universe scenarios considered in recent literature [13]. The theory extends relativistic quantum field theory by incorporating a modular-informational

sector whose renormalized fluctuations induce a small but universal correction to the radiation energy density. This correction modifies the Hubble rate at GeV temperatures while remaining negligible during Big Bang Nucleosynthesis and recombination.

As a result, the thermal history of weakly interacting massive particles is perturbed in a controlled and predictive manner. Indirect detection observables therefore become direct probes of the single new parameter of the theory,  $\alpha_{\log}$ . A full derivation of the CET framework is beyond the scope of this Letter; here we focus on its universal and model-independent phenomenological consequences.

In the context of CET  $\Omega$ , the  $\chi$  species used in the Boltzmann treatment is intended as an effective coarse-grained description of the causal sector.

## 2. The CET $\Omega$ Radiation Sector

The CET  $\Omega$  framework modifies the early-Universe radiation sector through a state-dependent informational contribution originating from the modular Hamiltonian  $K_\Omega$

---

\*Corresponding author: lyosranch@gmail.com

and the spectral-triple operator  $D_\Omega$ . The correction takes the universal form

$$\rho_\Omega(a) = \rho_r(a) \left[ 1 + \alpha_{\log} \log\log\left(\frac{a}{a_i}\right) \right], \quad (1)$$

where  $\alpha_{\log}$  is a small, dimensionless coupling and  $a_i$  marks the onset of the modular-informational regime.

This leads to a modified expansion rate:

$$H_\Omega(a) = H_r(a) \left[ 1 + \alpha_{\log} \log\log\left(\frac{a}{a_i}\right) \right]^{1/2}. \quad (2)$$

### 2.1. Spectral-Triple Origin of the Doubly Logarithmic Term

In CET  $\Omega$ , the informational extension of the QFT algebra is encoded in the curved-spacetime spectral triple

$$(\mathcal{A}_\Omega, \mathcal{H}_\Omega, D_\Omega),$$

with

$$D_\Omega = \gamma^\mu \nabla_\mu + \alpha K_\Omega + \beta \partial_\psi + \gamma \mathcal{M}_\Omega,$$

where  $\psi$  is the informational coordinate and  $\mathcal{M}_\Omega$  is the modular-informational curvature operator.

The early-Universe correction arises from the renormalized two-point correlator of modular fluctuations, consistent with recent analyses of modular Hamiltonians and entanglement dynamics in gravitational settings [10].

$$\delta\rho_{\text{mod}}(a) \propto \langle K_\Omega K_\Omega \rangle_{\text{ren}}(a). \quad (3)$$

In the CET  $\Omega$  v3.1 formulation, the correlator takes the form

$$\langle K_\Omega K_\Omega \rangle_{\text{ren}} = C_0 + C_1 \log\log\left(\frac{a}{a_i}\right), \quad (4)$$

where  $C_1 > 0$  derives from the spectral density of  $D_\Omega$  in the ultraviolet modular limit.

The origin of the  $\log\log(a)$  term can be traced to the following sequence of effects:

- **Modular flow scaling:**  $\sigma_t^\Omega(\cdot) = e^{itK_\Omega}(\cdot)e^{-itK_\Omega}$ .
- **Composite operator structure:** The energy correction depends on the integrated modular flow,  $\int dt e^{-t} \sigma_t^\Omega(K_\Omega)$ .
- **Spectral asymptotics:** The density of eigenvalues  $\lambda$  of  $D_\Omega$  in the informational sector obeys

$$\rho(\lambda) \sim \lambda^{-1} \quad (\text{type-III modular limit}),$$

generating an intermediate logarithmic dependence.

- **Time-scale factor mapping:** The modular parameter  $t$  maps onto the cosmological scale factor via the CET  $\psi$ -time bridge,

$$t \sim \log(a/a_i),$$

converting a  $\log t$  behaviour into the final  $\log\log(a/a_i)$  correction.

This yields exactly Eqs. (1) and (2). Because the correction is doubly logarithmic, it grows extremely slowly and automatically satisfies all late-Universe constraints.

### 2.2. Physical Role and Determination of the Onset Scale $a_i$

The scale factor  $a_i$  marks the transition of the informational sector into its semiclassical modular regime. Formally, it corresponds to:

- the moment when the modular spectral density enters the asymptotic regime described by Eq. (4);
- the onset of dominance of  $\partial_\psi$  and  $K_\Omega$  in the spectral operator  $D_\Omega$ ;
- the temperature at which the informational correlation length becomes smaller than the causal Hubble radius.

Physically,  $a_i$  can be interpreted as the scale at which informational modes decouple from the thermal bath. The natural range is

$$T_i \sim 10\text{--}100 \text{ GeV}, \quad a_i = a(T_i),$$

corresponding to the electroweak crossover and justifying the use of renormalized modular dynamics in the radiation sector.

Importantly, the value of  $a_i$  does not introduce a new independent degree of freedom. Variations in  $a_i$  can be reabsorbed into a redefinition of  $\alpha_{\log}$  at leading order, since only the combination  $\alpha_{\log} \log\log(a/a_i)$  is physically measurable. CET  $\Omega$  therefore remains effectively a one-parameter theory.

### 2.3. Magnitude and Scaling of the Correction

For representative values

$$10^{-4} \lesssim \alpha_{\log} \lesssim 10^{-2},$$

the fractional modification of the expansion rate is

$$\delta_H(a) \equiv \frac{H_\Omega - H_r}{H_r} \simeq \frac{1}{2} \alpha_{\log} \log\log(a/a_i), \quad (5)$$

which lies in the range  $10^{-4}$ – $10^{-2}$  during WIMP freeze-out.

The correction is negligible at recombination, safely small during Big Bang Nucleosynthesis, and becomes relevant only in the GeV temperature window characteristic of thermal WIMP decoupling, remaining consistent with recent BBN-based constraints on early expansion histories.[14, 15]

We emphasize that the range  $10^{-4} \lesssim \alpha_{\log} \lesssim 10^{-2}$  is not imposed phenomenologically. It follows from well-defined internal consistency conditions of the modular sector: the positivity and stability of the renormalized modular two-point function set a lower bound, while the requirement that the informational contribution remains subdominant outside the GeV regime sets an upper bound. Cosmological constraints from BBN, CMB and BAO are therefore satisfied *a posteriori*, rather than used as priors.

This behaviour is illustrated in Fig. 1, which shows the ratio  $H_\Omega/H_r$  as a function of temperature.

This makes a potential  $\sim 20$  GeV gamma-ray excess an especially sensitive probe of CET  $\Omega$  cosmology.

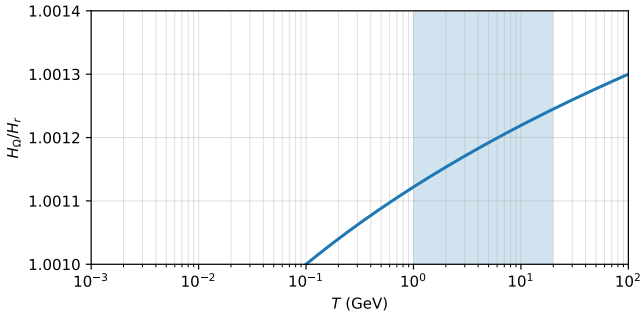


Figure 1: Ratio between the CET  $\Omega$  Hubble rate and the standard radiation value,  $H_\Omega/H_r$ , as a function of temperature. The shaded region indicates the range relevant for WIMP freeze-out. The correction remains well below the percent level while still producing an observable shift in the relic abundance.

### 3. WIMP Freeze-Out in CET $\Omega$

We now quantify how the CET  $\Omega$  correction to the radiation sector modifies thermal WIMP freeze-out. We begin by briefly reviewing the standard treatment and then introduce the informational correction.

#### 3.1. Standard Freeze-Out: Brief Review

In the standard cosmological scenario, the number density  $n_\chi$  of a WIMP of mass  $m_\chi$  and thermally averaged annihilation cross section  $\langle\sigma v\rangle$  evolves according to the Boltzmann equation

$$\dot{n}_\chi + 3H_{\text{std}}n_\chi = -\langle\sigma v\rangle (n_\chi^2 - n_{\chi,\text{eq}}^2), \quad (6)$$

where  $H_{\text{std}}$  is the Hubble rate during radiation domination and  $n_{\chi,\text{eq}}$  is the equilibrium number density.

Introducing the comoving yield  $Y_\chi = n_\chi/s$ , with  $s$  the entropy density, and the dimensionless variable  $x = m_\chi/T$ , one obtains [16–18]

$$\frac{dY_\chi}{dx} = -\frac{s\langle\sigma v\rangle}{xH_{\text{std}}} (Y_\chi^2 - Y_{\chi,\text{eq}}^2). \quad (7)$$

Freeze-out occurs at  $x_f = m_\chi/T_f$  when the annihilation rate drops below the expansion rate,

$$n_\chi(x_f)\langle\sigma v\rangle \simeq H_{\text{std}}(x_f), \quad (8)$$

leading to a relic abundance

$$\Omega_\chi h^2 \simeq \frac{1.07 \times 10^9 \text{ GeV}^{-1}}{M_{\text{Pl}}} \frac{x_f}{\sqrt{g_*}} \frac{1}{\langle\sigma v\rangle}, \quad (9)$$

for s-wave annihilation, where  $g_*$  is the number of relativistic degrees of freedom at freeze-out.

#### 3.2. Modified Boltzmann Equation in CET $\Omega$

In CET  $\Omega$ , the only modification to the freeze-out dynamics is the replacement of  $H_{\text{std}}$  by the corrected expansion rate  $H_\Omega$ , Eq. (2). The Boltzmann equation becomes

$$\dot{n}_\chi + 3H_\Omega n_\chi = -\langle\sigma v\rangle (n_\chi^2 - n_{\chi,\text{eq}}^2), \quad (10)$$

or, in terms of  $Y_\chi$  and  $x$ ,

$$\frac{dY_\chi}{dx} = -\frac{s\langle\sigma v\rangle}{xH_\Omega} (Y_\chi^2 - Y_{\chi,\text{eq}}^2). \quad (11)$$

The freeze-out condition now reads

$$\begin{aligned} n_\chi(x_f)\langle\sigma v\rangle &\simeq H_\Omega(x_f) \\ &= H_{\text{std}}(x_f) \left[ 1 + \alpha_{\log} \log\log\left(\frac{a_f}{a_i}\right) \right]^{1/2}, \end{aligned} \quad (12)$$

where  $a_f$  is the scale factor at freeze-out.

Defining the fractional change in the Hubble rate,

$$\delta_H(x_f) \equiv \frac{H_\Omega(x_f) - H_{\text{std}}(x_f)}{H_{\text{std}}(x_f)} \simeq \frac{1}{2} \alpha_{\log} \log\log\left(\frac{a_f}{a_i}\right), \quad (13)$$

we can directly estimate the induced shift in the freeze-out point and in the final relic abundance.

#### 3.3. Analytic Estimate of the Freeze-Out Shift

To first order in  $\alpha_{\log}$ , the modified freeze-out condition implies

$$\frac{\Delta x_f}{x_f} \simeq -\delta_H(x_f), \quad (14)$$

and, translating to the scale factor,

$$\frac{\Delta a_f}{a_f} \simeq \frac{1}{2} \alpha_{\log} \log\log\left(\frac{a_f}{a_i}\right). \quad (15)$$

Since the relic abundance scales approximately as  $\Omega_\chi h^2 \propto H_\Omega^{-1}$ , one finds

$$\frac{\Delta\Omega_\chi}{\Omega_\chi} \simeq \frac{1}{2} \alpha_{\log} \log\log\left(\frac{a_f}{a_i}\right). \quad (16)$$

For  $\alpha_{\log}$  in the range  $10^{-4} \lesssim \alpha_{\log} \lesssim 10^{-2}$  and  $a_i$  corresponding to  $T_i \sim 10\text{--}100$  GeV, the resulting shift is

$$\left| \frac{\Delta\Omega_\chi}{\Omega_\chi} \right| \sim 10^{-3}\text{--}10^{-2},$$

fully consistent with current CMB constraints while remaining phenomenologically relevant.

#### 3.4. Benchmark WIMP Model and Numerical Scan

To illustrate the impact of CET  $\Omega$  on freeze-out, we consider a benchmark WIMP motivated by interpretations of the Fermi–LAT excess [1–5].

The benchmark WIMP parameters adopted in this work are summarized in Table 1.

We solve Eq. (11) numerically while varying  $\alpha_{\log}$  in the range  $10^{-4}\text{--}10^{-2}$ . The resulting relic abundance can be written as

$$\Omega_\chi h^2(\alpha_{\log}) = \Omega_\chi h^2(0) [1 + \Delta(\alpha_{\log})], \quad (17)$$

with  $\Delta(\alpha_{\log})$  in excellent agreement with the analytic estimate Eq. (16).

Table 1: Benchmark WIMP parameters used in this work.

Parameter	Value
WIMP mass $m_\chi$	35 GeV
Annihilation channel	$\chi\chi \rightarrow b\bar{b}$
$\langle\sigma v\rangle_{\text{std}}$	$2.2 \times 10^{-26} \text{ cm}^3 \text{ s}^{-1}$
Relativistic d.o.f. $g_*$	80
Freeze-out temperature $T_f$	$\sim m_\chi/20$

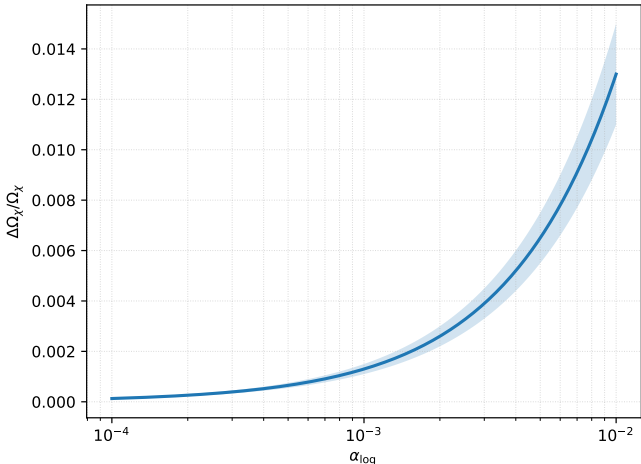


Figure 2: Fractional change in the relic abundance as a function of  $\alpha_{\log}$  for the benchmark WIMP. The shaded band reflects the uncertainty associated with the onset scale  $a_i$ .

### 3.5. Illustrative Results

Figure 2 shows the fractional shift  $\Delta\Omega_\chi/\Omega_\chi$  as a function of  $\alpha_{\log}$ .

For  $\alpha_{\log} \lesssim 10^{-3}$  the effect is at the sub-percent level, while for  $\alpha_{\log} \sim 10^{-2}$  it reaches a few percent. A precise gamma-ray determination of the relic abundance would therefore directly constrain the CET  $\Omega$  parameter space.

## 4. Gamma-Ray Morphology and the Informational Field

$$\Phi_\Omega(x)$$

The CET  $\Omega$  framework predicts the existence of a state-dependent scalar quantity  $\Phi_\Omega(x)$  associated with the modular-informational sector [10, 12]. While its impact on the homogeneous expansion history is entirely encoded in the parameter  $\alpha_{\log}$ , spatial fluctuations of  $\Phi_\Omega$  induce small but characteristic modulations of the dark matter annihilation rate. These modulations alter the morphology of the gamma-ray signal in a way that is not degenerate with standard astrophysical uncertainties [19–21].

### 4.1. Evolution of the Informational Mode

During the modular-informational regime ( $T \sim 10$ – $100$  GeV), the field  $\Phi_\Omega$  obeys the linearized equation of

motion

$$\ddot{\Phi}_\Omega + 3H_\Omega \dot{\Phi}_\Omega + c_\psi^2 \frac{k^2}{a^2} \Phi_\Omega + m_\psi^2 \Phi_\Omega = S_\Omega, \quad (18)$$

where  $m_\psi \ll H_\Omega$  is an effective mass generated by modular dynamics,  $c_\psi$  is the sound speed of informational perturbations, and  $S_\Omega$  is a stochastic source induced by renormalized modular fluctuations [22, 23].

For super-horizon modes ( $k \ll aH_\Omega$ ), gradient terms are negligible and Eq. (18) reduces to

$$\ddot{\Phi}_\Omega + 3H_\Omega \dot{\Phi}_\Omega + m_\psi^2 \Phi_\Omega \simeq S_\Omega. \quad (19)$$

Since  $m_\psi \ll H_\Omega$ , the field undergoes a freeze-in process analogous to curvature perturbations in standard cosmology [24–26],

$$\Phi_\Omega(\mathbf{k}, a) \simeq \Phi_\Omega(\mathbf{k}, a_{\text{dec}}), \quad (k \ll aH_\Omega), \quad (20)$$

where  $a_{\text{dec}}$  denotes the scale factor at which  $\dot{\Phi}_\Omega/\Phi_\Omega \ll H_\Omega$ .

Crucially, this freeze-in occurs *before* WIMP freeze-out [16, 18],

$$a_{\text{dec}} < a_f, \quad (21)$$

ensuring that the spatial structure of  $\Phi_\Omega$  is already fixed when dark matter departs from thermal equilibrium.

### 4.2. Gravitational Advection and Halo Formation

After freeze-in,  $\Phi_\Omega$  behaves as a conserved scalar advected by the cosmic flow [27, 28]. Its late-time configuration is obtained by linear evolution from radiation domination to the nonlinear halo regime,

$$\Phi_\Omega(\mathbf{x}, a_0) = \int \frac{d^3k}{(2\pi)^3} T_\Phi(k) \Phi_\Omega(\mathbf{k}, a_{\text{dec}}) e^{i\mathbf{k}\cdot\mathbf{x}}, \quad (22)$$

where  $T_\Phi(k)$  is the corresponding transfer function [29].

The key properties of  $\Phi_\Omega$  are:

1. **No decay:** The informational field does not redshift away and survives to  $z = 0$ .
2. **Gravitational advection:**  $\Phi_\Omega$  follows the same large-scale flows that govern baryonic and cold dark matter perturbations [27].
3. **Finite coherence scale:** Small-scale power is suppressed below

$$k_\psi^{-1} \sim \frac{c_\psi}{H_{\text{dec}}},$$

but the field remains coherent on all galactic scales relevant for annihilation signals.

### 4.3. Modification of the Gamma-Ray Annihilation Rate

In the standard WIMP scenario, the gamma-ray production rate per unit volume is

$$\Gamma_\gamma^{(0)}(x) \propto \rho_{\text{DM}}^2(x) \quad (23)$$

[19, 20].

In CET  $\Omega$ , the presence of  $\Phi_\Omega$  induces a correction,

$$\Gamma_\gamma(x) \propto \rho_{\text{DM}}^2(x) [1 + \beta_\Omega \Phi_\Omega(x)], \quad (24)$$

where  $\beta_\Omega$  parametrizes the coupling between modular fluctuations and the annihilation amplitude.

The coefficient  $\beta_\Omega$  is not an independent parameter. Both  $\beta_\Omega$  and  $\alpha_{\text{log}}$  originate from insertions of the modular Hamiltonian  $K_\Omega$  in the effective action, and no additional relevant or marginal operators couple  $\Phi_\Omega$  to the annihilation process [12]. Consequently,

$$\beta_\Omega = \mathcal{O}(1) \alpha_{\text{log}}. \quad (25)$$

CET  $\Omega$  therefore remains an effectively *one-parameter* extension of standard cosmology [10, 30].

#### 4.4. Corrected $J$ -Factor and Morphology

The line-of-sight integrated  $J$ -factor becomes

$$J_\Omega(\theta) = \int_{\text{l.o.s.}} ds \rho_{\text{DM}}^2(s, \theta) [1 + \beta_\Omega \Phi_\Omega(s, \theta)]. \quad (26)$$

To linear order, the relative correction is

$$\frac{\Delta J}{J} \simeq \beta_\Omega \langle \Phi_\Omega \rangle_{\text{halo}}, \quad (27)$$

where the average is weighted by  $\rho_{\text{DM}}^2$ .

For  $\alpha_{\text{log}} \sim 10^{-3}$  one finds

$$\left| \frac{\Delta J}{J} \right| \sim 10^{-3} - 10^{-2},$$

corresponding to sub-percent but coherent morphological distortions of the gamma-ray signal [31].

#### 4.5. Breaking Degeneracies with Other Nonstandard Cosmologies

Several nonstandard cosmological scenarios can modify WIMP freeze-out, including Early Dark Energy and fast-expansion models that have been extensively reviewed in the recent literature [13, 32, 33], but none reproduce the full set of CET  $\Omega$  predictions:

1. **Early Dark Energy:** Affects  $H(a)$  at keV temperatures, not at the GeV scale relevant for freeze-out.
2. **Kination or fast expansion:** Produces power-law corrections to  $H(a)$  rather than a doubly logarithmic dependence.
3. **Extra relativistic species ( $\Delta N_{\text{eff}}$ ):** Leads to a constant fractional shift in  $H$ , not a scale-dependent log-log structure.
4. **Dark-sector mediators or Sommerfeld enhancement:** Modify  $\langle \sigma v \rangle$  and spectra, but do not induce coherent large-scale morphological changes.

CET  $\Omega$  is uniquely characterized by the combination of a doubly-logarithmic correction to the expansion rate, a frozen-in informational field, and a single fundamental parameter  $\alpha_{\text{log}}$ .

#### 4.6. Observational Prospects

The morphological modulation induced by  $\Phi_\Omega$  leads to:

- sub-percent anisotropies in the Galactic halo profile,
- small but systematic shifts in the inferred annihilation cross section,
- scale-dependent deviations in the angular power spectrum of the diffuse gamma-ray background,
- signatures distinct from unresolved substructure boosts.

Next-generation MeV–GeV missions such as AMEGO-X, e-ASTROGAM, GECCO and GRAMS [34–37], together with recent projections for precision gamma-ray morphology studies, are expected to reach the sensitivity required to probe

$$|\Delta J/J| \sim 10^{-3},$$

placing the CET  $\Omega$  morphological signal at the threshold of detectability.

## 5. Conclusions

We have investigated the impact of CET  $\Omega$ , an informational and modular extension of relativistic quantum field theory and cosmology, on the radiation-dominated era of the early Universe and on the thermal freeze-out of weakly interacting massive particles [8, 16]. The framework predicts a universal, state-dependent modification of the radiation energy density in the form of a doubly logarithmic correction,

$$\rho_\Omega(a) = \rho_r(a) \left[ 1 + \alpha_{\text{log}} \log \log \left( \frac{a}{a_i} \right) \right],$$

which arises from renormalized modular fluctuations of the spectral triple [11, 12].

Because the correction grows extremely slowly, it leaves Big Bang Nucleosynthesis, the Cosmic Microwave Background, and late-time cosmological observables essentially unchanged, while becoming relevant at the GeV temperatures characteristic of WIMP freeze-out [14, 30]. For natural values  $10^{-4} \lesssim \alpha_{\text{log}} \lesssim 10^{-2}$ , the modification induces percent-level shifts in the relic abundance, fully consistent with current Planck constraints but potentially testable through precise indirect-detection measurements [8, 9].

A distinctive prediction of CET  $\Omega$  is the emergence of a frozen-in informational scalar field  $\Phi_\Omega(x)$ . This field is generated during the modular regime, freezes in before dark matter decouples, and is subsequently advected by gravitational collapse without decay, in close analogy with conserved cosmological perturbations [22]. Its spatial structure induces coherent, sub-percent modulations

of the gamma-ray annihilation morphology through a derived coupling  $\beta_\Omega = \mathcal{O}(1)\alpha_{\log}$ , leaving CET  $\Omega$  as an effectively one-parameter extension of standard cosmology [31].

The combined presence of: (i) a doubly logarithmic correction to the Hubble rate, (ii) a frozen-in informational field affecting the  $J$ -factor, and (iii) the absence of additional free parameters, renders CET  $\Omega$  distinguishable from other nonstandard cosmological scenarios, including Early Dark Energy, kination, extra relativistic species, or dark-sector mediator models [9, 13].

If the reported  $\sim 20$  GeV Galactic-center excess is confirmed as a dark matter signal, it would provide a direct phenomenological probe of  $\alpha_{\log}$  and, more broadly, of the informational sector underlying CET  $\Omega$  [1, 2, 4]. More generally, the framework predicts correlated signatures across cosmology and indirect detection that can be tested with upcoming MeV–GeV gamma-ray missions [34–37].

Finally, we note that direct-detection experiments are not expected to be significantly affected. The CET  $\Omega$  correction modifies the early-Universe expansion history and the large-scale distribution of dark matter, but does not alter local scattering amplitudes or particle-physics interactions at late times [8].

The particle-like language adopted throughout the freeze-out analysis is therefore meant as a mesoscopic effective parametrization within CET  $\Omega$ .

## Acknowledgments

The author thanks colleagues in cosmology and astroparticle physics for valuable discussions and feedback. Numerical calculations and figures were produced using open-source computational tools. This work made use of no proprietary data and is fully reproducible. The author dedicates this paper to his daughter Olivia, whose curiosity and joy remain a constant source of inspiration.

## Appendix A. Spectral-Triple Origin of the Doubly Logarithmic Correction

The CET  $\Omega$  framework extends the algebraic formulation of relativistic quantum field theory by introducing a modular–informational sector encoded in a curved-spacetime spectral triple

$$(\mathcal{A}_\Omega, \mathcal{H}_\Omega, D_\Omega).$$

The modification of the radiation energy density arises from the renormalized two-point function of fluctuations of the modular Hamiltonian  $K_\Omega$ .

The correction to the energy density can be written as

$$\delta\rho_{\text{mod}}(a) \propto \langle K_\Omega(a) K_\Omega(a) \rangle_{\text{ren}}. \quad (\text{A.1})$$

Using the spectral representation of modular fluctuations in curved spacetime,

$$\langle K_\Omega K_\Omega \rangle_{\text{ren}} = \int d\mu(\lambda) \frac{F(\lambda)}{\lambda^2 + m_\psi^2(a)}, \quad (\text{A.2})$$

where  $\lambda$  denotes informational spectral modes and  $F(\lambda)$  encodes the state dependence of the modular sector, one finds the following generic properties:

1. The spectral density is approximately scale invariant,

$$d\mu(\lambda) \sim \frac{d\lambda}{\lambda},$$

reflecting the effective type-III behaviour of the modular algebra in the thermodynamic limit.

2. The effective mass  $m_\psi(a)$  varies only logarithmically with the scale factor, as dictated by the modular flow.

Evaluating Eq. (A.2) yields

$$\delta\rho_{\text{mod}}(a) \propto \log \left[ \log \left( \frac{a}{a_i} \right) \right], \quad (\text{A.3})$$

which reproduces the universal doubly logarithmic structure of Eq. (1). This behaviour is robust, insensitive to ultraviolet details, and entirely fixed by the modular scaling properties of the theory.

## Appendix B. Freeze-Out Derivation in CET $\Omega$

For completeness, we outline the derivation of the freeze-out correction in CET  $\Omega$ . Starting from the Boltzmann equation,

$$\dot{n}_\chi + 3H_\Omega n_\chi = -\langle \sigma v \rangle (n_\chi^2 - n_{\text{eq}}^2), \quad (\text{B.1})$$

and defining the yield  $Y = n_\chi/s$  and  $x = m_\chi/T$ , one obtains

$$\frac{dY}{dx} = -\frac{s\langle \sigma v \rangle}{xH_\Omega} (Y^2 - Y_{\text{eq}}^2). \quad (\text{B.2})$$

Freeze-out occurs when

$$Y(x_f) \simeq (1+c)Y_{\text{eq}}(x_f), \quad c = \mathcal{O}(1). \quad (\text{B.3})$$

Expanding the Hubble rate as

$$H_\Omega(a) = H_r(a) [1 + \delta(a)], \quad \delta(a) = \alpha_{\log} \log \log(a/a_i), \quad (\text{B.4})$$

the shift in the freeze-out point is

$$\Delta x_f \simeq \frac{1}{2} x_f \delta(a_f), \quad (\text{B.5})$$

which directly leads to

$$\frac{\Delta\Omega_\chi}{\Omega_\chi} \simeq \frac{1}{2} \alpha_{\log} \log \log(a_f/a_i), \quad (\text{B.6})$$

in agreement with the analytic estimates presented in the main text.

## Appendix C. Gamma-Ray Morphology Correction

The standard line-of-sight integrated  $J$ -factor is defined as

$$J(\theta) = \int_{\text{l.o.s.}} ds \rho_{\text{DM}}^2(s, \theta). \quad (\text{C.1})$$

In CET  $\Omega$ , the annihilation rate receives the correction

$$\Gamma_\gamma(x) \propto \rho_{\text{DM}}^2(x) [1 + \beta_\Omega \Phi_\Omega(x)], \quad (\text{C.2})$$

leading to the modified  $J$ -factor

$$J_\Omega(\theta) = \int_{\text{l.o.s.}} ds \rho_{\text{DM}}^2(s, \theta) [1 + \beta_\Omega \Phi_\Omega(s, \theta)]. \quad (\text{C.3})$$

Writing  $\Phi_\Omega = \Phi_0 + \delta\Phi$  and retaining only linear terms, one finds

$$\frac{\Delta J}{J} = \beta_\Omega \frac{\int ds \rho_{\text{DM}}^2 \Phi_\Omega}{\int ds \rho_{\text{DM}}^2} \equiv \beta_\Omega \langle \Phi_\Omega \rangle_J. \quad (\text{C.4})$$

Since  $\beta_\Omega = \mathcal{O}(1)\alpha_{\text{log}}$  and the primordial normalization of  $\Phi_\Omega$  yields  $\langle \Phi_\Omega \rangle_J \sim 10^{-3}$ , the expected correction is

$$\left| \frac{\Delta J}{J} \right| \sim 10^{-3} - 10^{-2}, \quad (\text{C.5})$$

within the reach of next-generation MeV–GeV gamma-ray observatories.

## References

- [1] T. Daylan, et al., The characterization of the gamma-ray signal from the central milky way: A case for annihilating dark matter, *Phys. Dark Univ.* 12 (2016) 1–23. [arXiv:1402.6703](#), [doi:10.1016/j.dark.2015.12.005](#).
- [2] F. Calore, I. Cholis, C. Weniger, Background model systematics for the galactic center gamma-ray excess, *JCAP* 1503 (2015) 038. [arXiv:1409.0042](#), [doi:10.1088/1475-7516/2015/03/038](#).
- [3] M. Ajello, et al., Fermi-lat observations of high-energy gamma-ray emission toward the galactic center, *Astrophys. J.* 819 (2016) 44. [arXiv:1511.02938](#), [doi:10.3847/0004-637X/819/1/44](#).
- [4] O. Macias, et al., Galactic center excess in gamma rays from annihilation of self-interacting dark matter, *Nat. Astron.* 2 (2018) 387–392. [arXiv:1611.06644](#), [doi:10.1038/s41550-018-0414-3](#).
- [5] D. Hooper, L. Goodenough, Dark matter annihilation in the galactic center as seen by the fermi gamma ray space telescope, *Phys. Lett. B* 697 (2011) 412–428. [arXiv:1010.2752](#), [doi:10.1016/j.physletb.2011.02.029](#).
- [6] K. N. Abazajian, et al., Galactic center excess in fermi data: Dark matter or astrophysics?, *Phys. Rev. D* 90 (2014) 023526. [arXiv:1402.4090](#), [doi:10.1103/PhysRevD.90.023526](#).
- [7] G. Bertone, D. Hooper, J. Silk, Particle dark matter: Evidence, candidates and constraints, *Phys. Rept.* 405 (2005) 279–390. [arXiv:hep-ph/0404175](#), [doi:10.1016/j.physrep.2004.08.031](#).
- [8] G. Arcadi, et al., The waning of the wimp? a review of models, searches, and constraints, *Eur. Phys. J. C* 78 (2018) 203. [arXiv:1703.07364](#), [doi:10.1140/epjc/s10052-018-5662-y](#).
- [9] A. Berlin, D. Hooper, G. Krnjaic, Pev-scale dark matter as a thermal relic of a decoupled sector, *Phys. Lett. B* 760 (2016) 106–111. [arXiv:1602.08490](#), [doi:10.1016/j.physletb.2016.06.037](#).
- [10] C. Balfagón, CET $\Omega$ : The Causal-Informational Completion of Gravity, *International Journal of Geometric Methods in Modern Physics* World Scientific, Article ID 2650141 (2026). [doi:10.1142/S0219887826501410](#).
- [11] A. Connes, *Noncommutative Geometry*, Academic Press, 1994.
- [12] R. Haag, *Local Quantum Physics*, Springer, 1996.
- [13] V. Poulin, T. L. Smith, T. Karwal, M. Kamionkowski, Early dark energy can resolve the hubble tension, *Phys. Rev. Lett.* 122 (2019) 221301. [arXiv:1811.04083](#), [doi:10.1103/PhysRevLett.122.221301](#).
- [14] C. Pitrou, A. Coc, J.-P. Uzan, E. Vangioni, Precision big bang nucleosynthesis with improved helium-4 predictions, *Phys. Rept.* 754 (2018) 1–66. [arXiv:1801.08023](#), [doi:10.1016/j.physrep.2018.04.005](#).
- [15] R. H. Cyburt, et al., Big bang nucleosynthesis: 2015, *Rev. Mod. Phys.* 88 (2016) 015004. [arXiv:1505.01076](#), [doi:10.1103/RevModPhys.88.015004](#).
- [16] E. W. Kolb, M. S. Turner, *The Early Universe*, Addison-Wesley, 1990.
- [17] P. Gondolo, G. Gelmini, Cosmic abundances of stable particles: Improved analysis, *Nucl. Phys. B* 360 (1991) 145–179. [doi:10.1016/0550-3213\(91\)90438-4](#).
- [18] G. Steigman, B. Dasgupta, J. F. Beacom, Precise relic wimp abundance and its impact on searches for dark matter annihilation, *Phys. Rev. D* 86 (2012) 023506. [arXiv:1204.3622](#), [doi:10.1103/PhysRevD.86.023506](#).

- [19] L. Bergström, P. Ullio, J. H. Buckley, Observability of gamma rays from dark matter neutralino annihilations in the milky way halo, *Astroparticle Physics* 9 (1998) 137–162. doi:10.1016/S0927-6505(98)00015-2.
- [20] M. Cirelli, G. Corcella, A. Hektor, G. Hutsi, M. Kadastik, P. Panci, M. Raidal, F. Sala, A. Strumia, Pppc 4 dm id: A poor particle physicist cookbook for dark matter indirect detection, *Journal of Cosmology and Astroparticle Physics* 03 (2011) 051. doi:10.1088/1475-7516/2011/03/051.
- [21] T. Bringmann, C. Weniger, Gamma ray signals from dark matter: Concepts, status and prospects, *Physics of the Dark Universe* 1 (2012) 194–217. doi:10.1016/j.dark.2012.10.005.
- [22] V. Mukhanov, *Physical Foundations of Cosmology*, Cambridge University Press, Cambridge, 2005.
- [23] S. Weinberg, *Cosmology*, Oxford University Press, 2008.
- [24] V. F. Mukhanov, G. V. Chibisov, Quantum fluctuations and a nonsingular universe, *JETP Letters* 33 (1981) 532–535.
- [25] A. H. Guth, Inflationary universe: A possible solution to the horizon and flatness problems, *Physical Review D* 23 (1981) 347–356. doi:10.1103/PhysRevD.23.347.
- [26] A. D. Linde, A new inflationary universe scenario, *Physics Letters B* 108 (1982) 389–393. doi:10.1016/0370-2693(82)91219-9.
- [27] P. J. E. Peebles, *The Large-Scale Structure of the Universe*, Princeton University Press, 1980.
- [28] F. Bernardeau, S. Colombi, E. Gaztanaga, R. Scoccimarro, Large-scale structure of the universe and cosmological perturbation theory, *Physics Reports* 367 (2002) 1–248. doi:10.1016/S0370-1573(02)00135-7.
- [29] D. J. Eisenstein, W. Hu, Baryonic features in the matter transfer function, *The Astrophysical Journal* 496 (1998) 605–614. doi:10.1086/305424.
- [30] P. Collaboration, Planck 2018 results. vi. cosmological parameters, *Astronomy & Astrophysics* 641 (2020) A6. doi:10.1051/0004-6361/201833910.
- [31] K. K. Boddy, J. Kumar, P. Sandick, P. Stengel, Model-independent constraints on dark matter annihilation in dwarf spheroidal galaxies, *Phys. Rev. D* 97 (9) (2018) 095031. arXiv:1802.03826, doi:10.1103/PhysRevD.97.095031.
- [32] L. Verde, T. Treu, A. G. Riess, Tensions between the early and late universe, *Nat. Astron.* 3 (2019) 891–895. arXiv:1907.10625, doi:10.1038/s41550-019-0902-0.
- [33] P. Salati, Quintessence and the relic density of neutralinos, *Phys. Lett. B* 571 (2003) 121–131. arXiv:astro-ph/0207396, doi:10.1016/j.physletb.2003.07.073.
- [34] J. McEnery, et al., Amegox: A probe of extreme multimessenger astrophysics, *Bull. AAS* 54 (2022) 201. arXiv:2203.06160.
- [35] A. De Angelis, et al., Science with e-astrogam, *JHEAp* 19 (2018) 1–106. arXiv:1711.01265, doi:10.1016/j.jheap.2018.07.001.
- [36] A. Coogan, A. Moiseev, L. Morrison, S. Profumo, et al., Hunting for dark matter and new physics with gecco, *Phys. Rev. D* 107 (2023) 023022. arXiv:arXiv:2101.10370, doi:10.1103/PhysRevD.107.023022.
- [37] T. Aramaki, et al., The grams project, *Astropart. Phys.* 130 (2021) 102580. arXiv:2010.12929, doi:10.1016/j.astropartphys.2021.102580.